OPEN ACCESS
Journal of Multidisciplinary Applied Natural Science Vol. 6 No. 1 (2026) https://doi.org/10.47352/jmans.2774-3047.339
Check for updates
Research Article

Biological and Photocatalytic Activities of Magnesium Oxide Nanoparticles Prepared from Seawater Bittern by Electrochemical Method

Hanif Amrulloh*, Chairul Ichsan, Wasinton Simanjuntak, Oman Zuas, Yehezkiel Steven Kurniawan, and Claudia Maria Simonescu

Received : February 15, 2025	Revised : August 20, 2025	Accepted : October 25, 2025	Online : January 1, 2026

Abstract
The present study aims to prepare magnesium oxide (MgO) nanoparticles from seawater bittern using an electrochemical method to evaluate their application as antioxidant, antimicrobial, and photocatalytic agents. The synthesis of nanomaterial was performed at room temperature, employing graphite and nickel as anode and cathode, respectively, without any pH adjustment. Spectroscopic analysis determined that the optical band gap of MgO nanoparticles was 4.814 eV. The XRD patterns show hexagonal single cubic phase MgO matched with JCPDS Card No 78-0430. Electron microscopic analysis demonstrated the appearance of MgO nanoparticles in spherical morphology with 30–50 nm in particle size. Based on the maximum inhibition concentration (MIC), it was found that the MgO nanoparticles has good antibacterial activity against *Staphylococcus aureus*, *Enterococcus faecalis*, *Escherichia coli*, and *Shigella dysenteriae* bacteria (MIC values: 220−480 μg mL^{-1}), and much stronger antifungal activity against *Aspergillus flavus*, *Aspergillus niger*, and *Candida albicans* (MIC values: 62.5–115 μg mL^{-1}). Methylene blue and rhodamine B dyes were degraded by MgO nanoparticles with strong photocatalytic activity when they were exposed to visible light and achieved 97% and 95% degradation, respectively. This study demonstrates that MgO nanoparticles can be effectively applied in industries like wastewater treatment and nanomedicine.

Keywords: antimicrobial, bittern, magnesium oxide nanoparticles, photocatalytic

1. INTRODUCTION

Magnesium oxide MgO (nanoparticles) are environmentally friendly, economically promising, and industrially significant nanomaterials due to their unique physicochemical properties [1]-[3]. Based on these properties, MgO finds numerous applications such as a semiconductor material [4], a catalyst for organic compound synthesis [5], an adsorbent for organic and inorganic waste [6], a photocatalyst [7], and a refractory material [8]. MgO nanoparticles also exhibit excellent antibacterial [9], antifungal [10], anticancer [11], and antioxidant [9] properties. Several researchers have synthesized metal oxide nanoparticles using various methods, including sol-gel [12], sonochemistry [13], co-precipitation [14], green chemistry [15], chemical reduction [16], and electrochemical [17]. Among them, the electrochemical method attracts interest to researchers for synthesizing metal and metal oxide nanoparticles because it can be performed at low temperatures and pressures [18].

The electrochemical method is widely used for preparing magnesium oxide (MgO) or magnesium hydroxide with seawater bittern as a magnesium ion source. Amrulloh et al. [17] synthesized nano-sized MgO based on seawater and bittern obtained from the local salt industry in Pamekasan, Madura, Indonesia, using the electrochemical method. The electrochemical process was carried out in a two-compartment electrochemical cell with a fixed potential of 18 V for 4 h at ambient temperature and without adjusting the initial pH. The obtained solid was identified as $Mg(OH)_2$, which was then converted to MgO through calcination treatment at 500 °C for 4 h. Characterization results showed that the produced MgO material was spherical in shape with particle sizes ranging from 60 to 100 nm, indicating successful synthesis of MgO nanoparticles [17].

MgO nanoparticles have a potential application as an antimicrobial and photocatalyst for the degradation of wastewater under UV or visible radiation. Amrulloh et al. [10] showed that the antioxidant activity increases proportionally directly with MgO nanoparticle concentration tested by the

Table 1. Composition of primary elements in bittern.

Ions (g L^{-1})	Na^+	K^+	Mg^{2+}	Ca^{2+}
Bittern	17.31	57.57	53.37	30.15

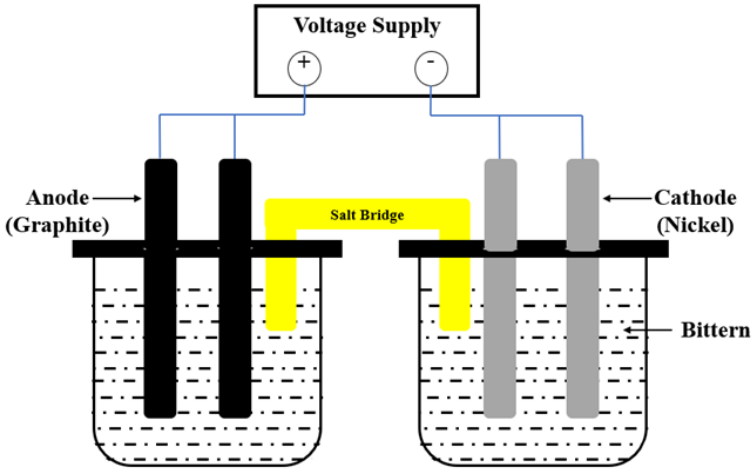

Figure 1. Schematic process of the electrochemical synthesis of MgO nanostructure.

DPPH free radical scavenging method. Antibacterial activity against *Staphylococcus aureus*, *Enterococcus faecalis*, *Escherichia coli*, and *Shigella dysenteriae* shows promising minimum inhibitory concentration (MIC) value of 250 µg mL^{-1}. Antifungal activity against *Aspergillus flavus*, *Aspergillus niger*, and *Candida albicans*, observed the lowest MIC against *C. albicans* (62.5 µg m L^{-1}) [10]. Nguyen et al. [19] studied the antimicrobial effect of MgO nanoparticles against *Pseudomonas aeruginosa*, *S. aureus*, MRSA, *C. albicans*, *C. albicans FR*, *Candida glabrata*, and *C. glabrata ER*. The MIC of MgO nanoparticles varied from 500 µg mL^{-1} to 1200 µg mL^{-1} and the minimal lethal concentration (MLC) of MgO nanoparticles at 90% killing varied from 700 to 1,400 µg mL^{-1} against the pathogenic bacteria and yeasts tested [19].

On the other hand, Kuruthukulangara and Asharani [20] reported the photocatalytic performance of MgO nanoparticles for rhodamine B degradation under UV light exposure. The MgO nanoparticles prepared by a one-pot process and the optical bandgap determined was 4.71 eV. The experimental results were consistent with first-order kinetics with 95% degradation. Pachiyappan et al. studies the photocatalytic properties of cubic crystal MgO nanoparticles for methylene blue (MB) and rhodamine B (RhB) dyes degradation. The optical band gap of MgO nanoparticles used was calculate and found to be 4.71 eV. The photocatalytic dye degradation was studied under visible light irradiation. The experimental data fitted first-order kinetics, and around >95% degeneration of both dyes was achieved by photocatalysis using synthesized MgO nanoparticles [20]. To the best of our knowledge, the application of MgO nanoparticles prepared from natural seawater bittern source through an electrochemical method for the antioxidant, antimicrobial, and photocatalytic dyes degradation has not been reported yet. Here, we investigated the biological and photocatalytic performance of the electrochemically synthesized MgO nanoparticle for the antimicrobial against the selected microbial and the degradation of MB and RhB.

2. MATERIALS AND METHODS

2.1. Materials

The bittern sample was obtained from a salt farm in Pamekasan, Madura Island, Indonesia. Other chemicals, e.g., gelatin powder, sodium chloride (NaCl), sulfuric acid (H_2SO_4), 2,2-diphenyl-1-picrylhydrazyl (DPPH), ascorbic acid, Tris-HCl buffer, ethanol, dimethyl sulfoxide (DMSO), resazurin sodium salt, MB, and RhB were of analytical grade purchased from Sigma-Aldrich Reagent Pte. Ltd., Singapore. All chemicals were used without any further purification.

2.2. Methods

2.2.1. Preparation of MgO Nanoparticles

The bittern sample was obtained from Pamekasan, Madura, Indonesia. The concentration of Mg^{2+}, together with other main cations in bittern, were analyzed using inductively coupled plasma-optical emission spectroscopy (715 ES, Variants). Table 1 shows that the content of Mg^{2+} ions in bittern is 53.37 g L^{-1} (2.22 mol L^{-1}). Prior to electrochemical experiments, the bittern was diluted with distilled water to adjust the concentration of Mg^{2+} in the range of 0.28–2.22 mol L^{-1}.

The preparation of MgO nanoparticles was conducted in a similar manner to that previously described in Amrulloh et al [17][21][22]. The electrochemical process employed a two-compartment electrochemical cell connected by a salt bridge (gelatin and NaCl suspension) with graphite and nickel as the cathode and anode, respectively. The schematic process of the electrochemical method is shown in Figure 1. Bittern samples were diluted four times with deionized water without any pH adjustment, and then the electrolysis process was performed at 18 V for 4h at room temperature. 1 mL of 0.1 M H_2SO_4 was added to the cathode solution for decarboxylation. The mixed solution was homogenously stirred at 120–600 rpm for 2 h. The resulting solid at the cathode was filtered and washed three times with deionized water. The solid sample was dried at 110 °C and then calcined at 500 °C for 4 h in a muffle furnace to produce MgO powder.

2.2.2. MgO Nanoparticles Characterization

The synthesized MgO nanoparticles were characterized with a UV-visible spectrophotometer (Analytic Jena Specord 200 Plus) to analyze the optical properties of the synthesized MgO nanoparticles. The diffractogram of MgO nanoparticles was recorded with continuous scanning for 2° min^{-1} by using an X-ray diffraction spectrometer (XRD, Expert Pro PANAnalytical) with Cu Kα radiation at 1.5406 Å (40 kV and 30 mA). Scanning electron microscope couplied with energy dispersive X-ray (SEM-EDX, FEI Inspect-S50) and transmission electron microscope (TEM, JEOL JEM-1400) analyses were conducted to determine the elemental composition and visualize the morphology and size of MgO nanoparticles. The average particle size was determined by the particle size analyser (PSA, Horiba SZ 100z).

2.2.3. Biological Activity Test

2.2.3.1. Antioxidant

Antioxidant activity of MgO nanoparticles and MgO nanoparticles standard was evaluated through DPPH radical testing in accordance with the

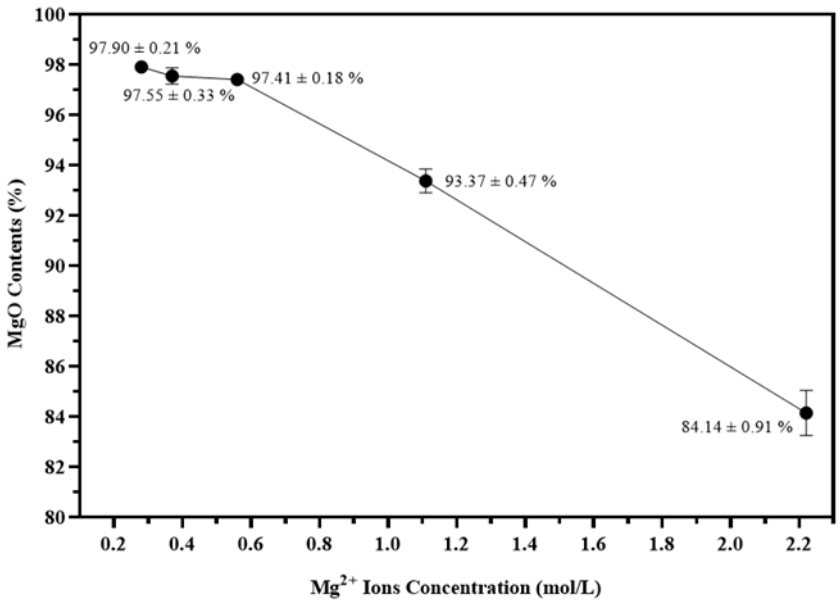

Figure 2. Effect of dilution of bittern on the MgO contents.

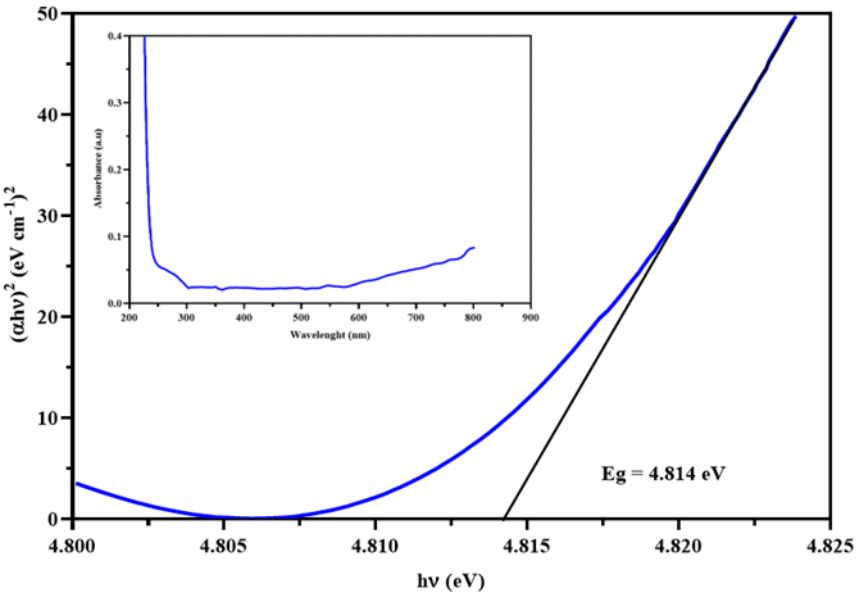

Figure 3. Tauc plot of MgO nanoparticles.

procedure described by Das et al. [9], using ascorbic acid as reference. A DPPH 0.1 mM solution was prepared by dissolving it in ethanol. 1 mg of ascorbic acid was dissolved in 1 mL of methanol. Dilution was carried out to make a standard solution of ascorbic acid with different concentrations (50–500 µg/mL). For each tube containing a standard solution of ascorbic acid (200 µL), 1 mL of 0.1 mM DPPH solution was added and followed by the addition of 800 µL 50 mM Tris-HCl buffer (pH 7.4). The final volume is adjusted to 4 mL using ethanol. Stock solutions of the prepared MgO nanoparticles and the standard MgO nanoparticles were prepared by dissolving 1 mg of each sample in 1 mL of DMSO.

Different aliquots of stock solution (50–500 µg) was added to separate tube, and the final volume was adjusted to 2 mL using ethanol. A total of 1 mL of 0.1 mM DPPH solution and 800 µL 50 mM Tris-HCl buffer (pH 7.4) was added to each tube. The control was made by mixing 1 mL DPPH 0.1 mM, 800 µL 50 mM Tris-HCl buffer (pH 7.4), and 2 mL ethanol. Absorbance was recorded after incubation for 30 min at room temperature, measured by an UV -vis spectrophotometer at 517 nm. The percentage of antioxidant activity (AA %) was calculated using the following Equation (1) [10].

$$(AA\%) = \frac{control\ absorbance - sample\ absorbance}{control\ absorbance}\ x\ 100\ \% \quad \textbf{(1)}$$

The mean and standard deviation (SD) were calculated based on triplicate measurements.

2.2.3.2. Antibacterial and Antifungal

2.2.3.2.1. *Microorganism and Inoculum Preparation*

The antibacterial activity of MgO nanoparticles and the standard was evaluated against both Gram-positive (*S. aureus* and *E. faecalis*) and Gram-negative (*E. coli* and *S. dysenteriae*) obtained from the microbiology laboratory of Airlangga University. The fungal cultures of *A. flavus*, *A. niger*, and *C. albicans* were obtained from the microbiology laboratory of Airlangga University. Bacterial and fungal cultures for testing were cultivated on nutrient agar (NA), tilted by selecting a colony from the Mueller-Hinton agar plate (MHA) after 24 h. For standardized populations, a single bacterial or fungal colony was selected and transferred using a sterilized loop to the Mueller-Hinton (MHB) broth, followed by continuous shaking at 100 rpm at 37 °C overnight. For the test of antibacterial and antifungal activity, the optical density of bacterial or fungal suspension was maintained at the 0.5 MacFarland standard by adding sterilized MHB. Thus, the inoculum consists of several bacteria or fungi around 10^6–10^7 CFU mL^{-1}.

2.2.3.2.2. *MIC Determination*

To determine the MIC, the resazurin microtiter assay was utilized. This method was chosen since it is considered as the most rapid and inexpensive way to screen several microorganism isolates at the same time, and provides satisfying results [23]-[25]. The resazurin solution was prepared by dissolving a 270 mg tablet of resazurin in 40 mL of sterile distilled water. The test was carried out in 96-well plates under aseptic conditions. A volume of 100 µL of the sample containing 600 µg mL^{-1} was transferred into the well of the plate. Afterwards, 50 µL of bacterial or fungal suspension was added to all other wells, and the tested sample was serially diluted. Subsequently, 10 µL of resazurin solution was added to each well. To prevent dehydration, the plates were wrapped with film and incubated at 37 ° C for 24 h. The color change was visually observed. A blue to pink color change was considered indicating cell growth. MIC was recorded at the lowest concentration where a color change occurred. Streptomycin (antibacterial) and ketoconazole (antifungal) (10 µg/500 µL) served as a positive control, whereas a mixture of sterile distilled water and DMSO solvent with nutrient broth were used as the negative controls.

2.2.4. *Photocatalytic Test*

A stock dye (MB and RhB) solution of 100 ppm was prepared by dissolving 100 mg of dye in 1 L of double-distilled water. The standard flask was kept for complete mixing by using magnetic stirrer. From the stock solution, 100 mL standard solutions of required concentrations (5–20 ppm) were prepared. The photocatalytic study for MB and RhB degradation according to Pachiyappan et al. [26]. In 100 mL of MB and RhB dye solution with a defined concentration (5–20 ppm), 100–500 mg of MgO nanoparticles were disseminated and subjected to visible light while swirling continuously. Withdrawing a certain volume of the exposed solution (10 mL), every 15 min, was used to measure the absorbance spectra of the samples. By centrifuging the solution, we were able to separate the MgO nanoparticles and evaluate their deterioration. A spectrophotometer at 664 and 554 nm was used (MB and RhB, respectively) to evaluate the degradation rate of the dye. Equation (2) was used to calculate the percentage of dye degradation;

$$\%\ Degradation = \left(\frac{C_i - C_e}{C_i}\right) x100\% \quad (2)$$

where *Ci* and *Ce* (mg L^{-1}) are the initial and equilibrium metal concentrations, respectively, and V is volume of solution taken.

3. RESULTS AND DISCUSSIONS

3.1. *Characterization of MgO Nanoparticles*

Figure 2 shows the effect of shows the effect of dilution of bittern on the purity of MgO produced,

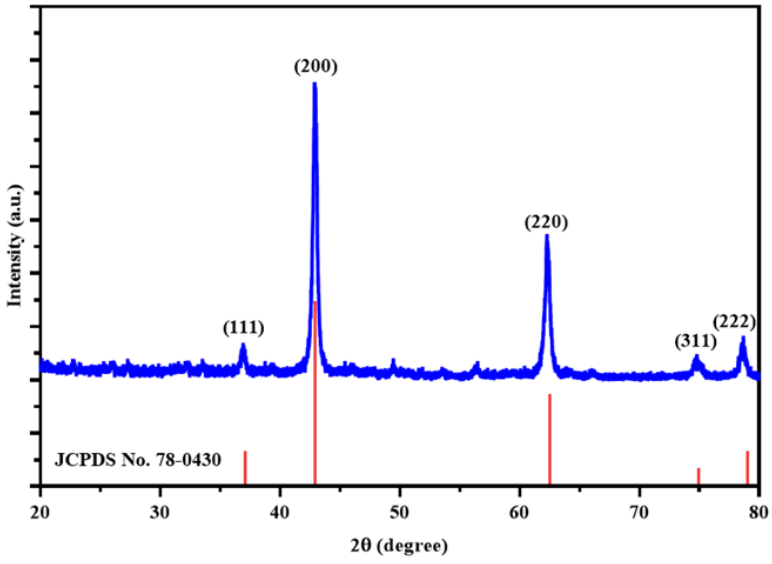

Figure 4. XRD diffractogram of MgO nanoparticles.

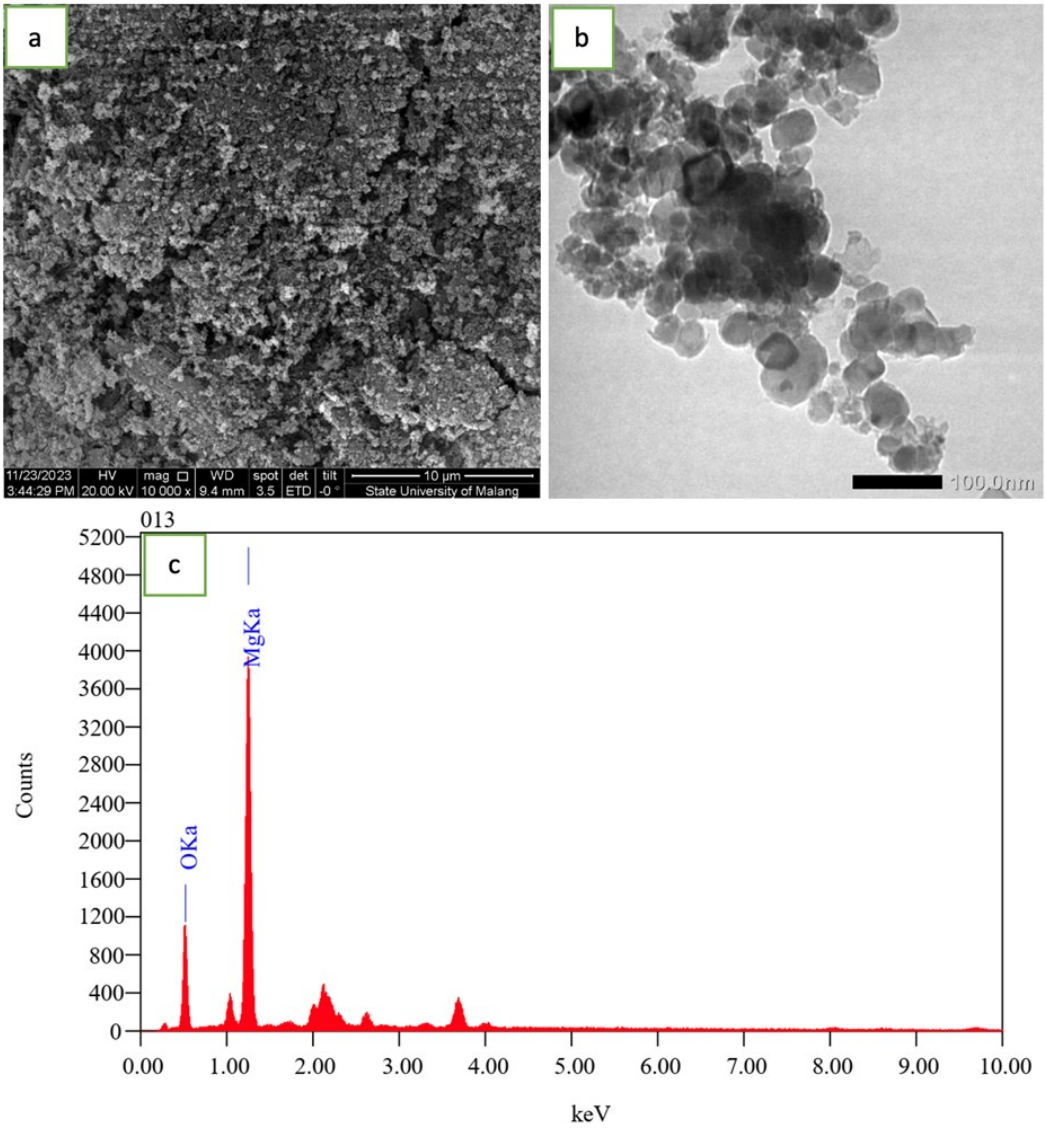

Figure 5. (a) SEM, (b) TEM, and (c) EDX profiles of MgO nanoparticles.

showing that dilution led to increased purity of the product. The best result (the purity of 97.41 %) was obtained by diluting the bittern four times (0.56 mol L^{-1} ion Mg^{2+}).

3.1.1. UV-vis Spectroscopy

The optical characteristics of MgO nanoparticles have been evaluated based on the double-beam UV-vis spectrophotometer examination by observing the absorption spectrum. The band gaps of the MgO nanoparticles were calculated using Tauc's plot (Eq. 3 and Figure 3) [27].

$$(\alpha h\nu)^{1/2} = A\,(h\nu - E_g) \quad (3)$$

where hv denotes the energy of the photon that struck the material, α denotes the absorption coefficient, A denotes a constant, Eg denotes the band gap energy (eV), and n = 1/2 for direct transitions that are permitted, as well as n = 2 for indirect transitions, are also mentioned. The MgO nanoparticle's band gap was found to be 4.814 eV. Kumar et al. [28] prepared MgO nanoparticles using tea extract under green chemistry route. The band gap of the prepared MgO nanoparticles was estimated at 4.21 eV.

3.1.2. XRD

XRD investigation determines the crystalline nature of the nanoparticles. Figure 4 shows the XRD diffractogram of the standard and the synthesized product. There are five typical diffraction peaks at 36.58°, 42.63°, 62.4°, 74.8°,

and 78.6°, indicating the presence of cubic MgO, and the peaks can be assigned to a pure phase of periclase MgO and have Miller indices as following (111), (200), (220), (311), and (222), which are in good agreement with the standar JCPDS card number 78-0430 [29]. The crystal size of the synthesized MgO nanoparticles was calculated from the Debye-Scherer equation (Eq. 4).

$$D\ (Å) = k\lambda / \beta \cos\theta \qquad (4)$$

where D is crystal size, β is full width at half maximum of the peak (FWHM), λ represents X-ray wavelength (1.54 Å), and K is the shape factor, which is always close to unity (0.9) [30]. Accordingly, the crystalline size of MgO nanoparticles created can now be expected to be around 13.561 nm.

3.1.3. SEM, TEM, and EDX

SEM characterization exhibited a rough spherical shape of MgO nanoparticles synthesized (Figure 5(a)). This indicates the homogeneity of the nanoparticles during the preparation of the MgO nanoparticles. The SEM images of MgO nanoparticles synthesized by *Moringa oleifera* eaf extract showed smiliar agglomerated spherical morphology [10]. The MgO nanoparticles made using the combustion method exhibited agglomerated roughly spherical shape [31]. Figure 5(b) shows a TEM micrograph of MgO nanoparticles at a scale of 100 nm. The average diameter of the MgO nanoparticles ranges from 7 to 65 nm. The TEM analysis revealed the irregular spherical morphology of MgO nanoparticles, consistent with the SEM dan XRD observations. TEM analysis of MgO nanoparticles synthesized from date pit extract showed a nanograin with a 14.0 nm mean size [32]. The average size of MgO nanoparticles synthesized using *Moringa oleifera* leaf extract was determined to be 35 nm in TEM studies [33]. The EDX result is shown in Figure 5 (c) revealing that the nanoparticles were composed of Mg and O in a molar rasio of about 1:1, they should be attributed to MgO.

3.1.4. Particle Size Distribution

To gain more insight regarding the particle size of the MgO nanoparticles produced, the particle size distribution of the sample was determined using the PSA technique. As displayed by the PSA result presented in Figure 6, the particle sizes of the synthesised MgO nanoparticles are in the range of 25 to 60 nm. Refering to the general definition of nanomaterial as the material with the particle size in the range of 1–100 nm, the PSA result confirms the successful preparation of MgO nanoparticles [34]. Another interesting result with respect to the result of PSA is that the distribution of particles of the NS -MgO synthesised practically follows a normal

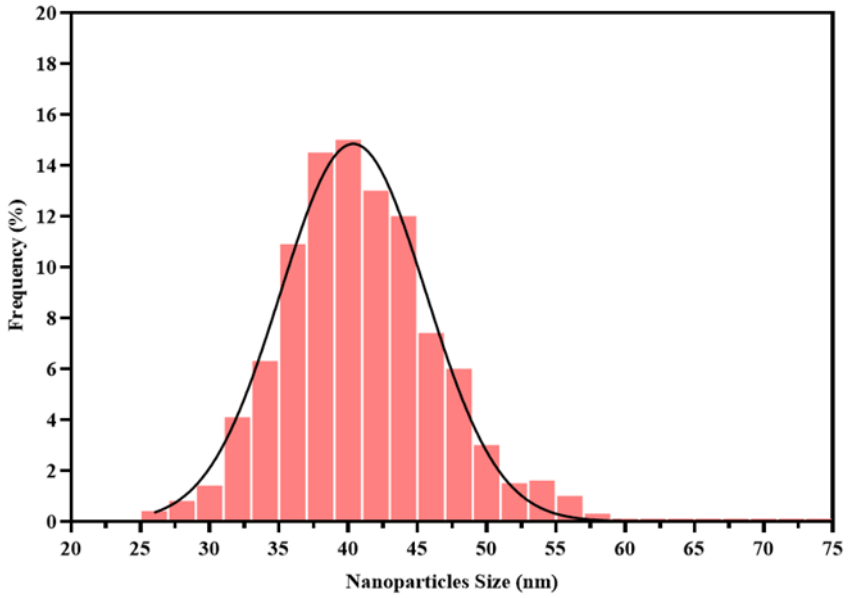

Figure 6. Particle size distribution of MgO nanoparticles.

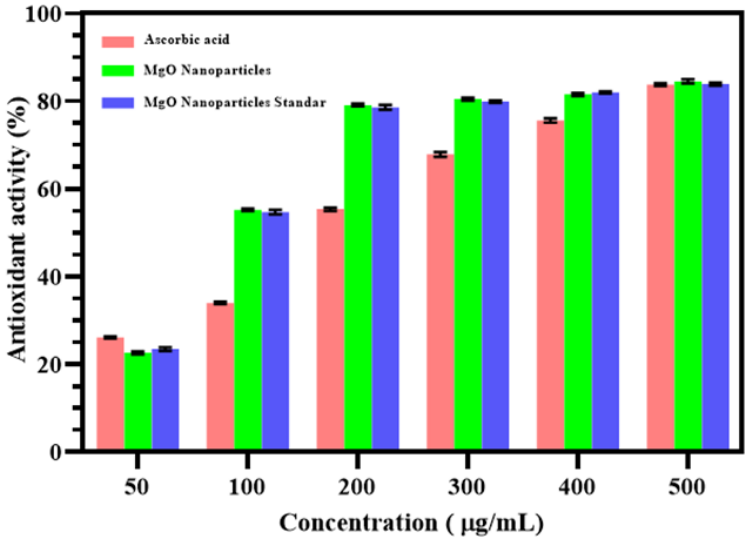

Figure 7. Antioxidant activity of MgO nanoparticles synthesized and MgO nanoparticles standard with ascorbic acid as a positive control.

distribution pattern. In this regard, it can be observed that most of the particles have a size in the range of 35 to 45 nm.

3.2. Bioactivity Test

3.2.1. Antioxidant Activity

In this study, the antioxidant activity of synthesized MgO nanoparticles and MgO nanoparticles standard was assessed by DPPH method using ascorbic acid as a positive control. This method, which is based on the free radical capture activity of DPPH, is often applied to study the antioxidant activity of nanoparticle materials [35]. The experimental results, showing a general trend of increased antioxidant activity of the samples as their concentrations increased, are presented in Figure 7. The most interesting result is that the activity of the synthesized MgO nanoparticles is very close to that of standard MgO nanoparticles. This particular finding demonstrates that the method developed in this current study for MgO nanoparticle's synthesis is very promising for the production of nanomaterials. It should also be mentioned that the results obtained in this study are in agreement with the results reported by others using nano-size ZnO [36], CuO [37], and MgO [9].

3.2.2. Antibacterial and Antifungal Activity

Antibacterial activity of MgO nanoparticles synthesized and MgO nanoparticles standard was evaluated against Gram-positive bacteria (*S. aureus* and *E. faecalis*) and Gram-negative (*E. coli* and *S. dysenteriae*) clinically isolated in vitro. The evaluation was carried out using the method of resazurin microtiter assay plate and the antibacterial activities of the samples are compiled in Figure 8. As can be seen in Figure 8, the MIC values of MgO nanoparticles synthesized for the four bacteria are in the range of 220−480 µg mL^{-1}, and comparable to those observed for the MgO nanoparticles standard (275−525 µg mL^{-1}). Overall, the MgO nanoparticles are more effective in combating *E. coli*, and *S. dysenteriae*, which are Gram-negative bacteria. Different antibacterial activity against gram-positive and gram-negative bacteria is most likely related to the structure of the cell walls of the bacteria. Gram-positive bacteria have a thick layer of peptidoglycan without an outer membrane and contain teichoic acid. In contrast, Gram-negative bacteria have a thin layer of peptidoglycan with an outer membrane that contains lipopolysaccharides. Because of this difference, each type of bacteria shows a different sensitivity [19].

The method of resazurin microtiter assay plate was also applied to evaluate the antifungal activity of the samples against *A. flavus*, *A. niger*, and *C. albicans*, as shown in Figure 9. As seen in Figure 9, based on their MIC values, MgO nanoparticles synthesized and NS-MgO standard exhibit

comparable effectivity, with the MIC values against *A. flavus*, *A. niger,* and *C. albican* are around 110, 115, and 62,5 µg mL^{-1}, respectively. Based on these MIC values, it can be inferred that the NS-MgO samples have better activity against *C. albican*, compared to the AEMOL, but against *A. flavus*, and *A. niger*, the opposite is true. With respect to the bioactivities investigated, another important finding that should be noted is that the NS-MgO is more effective as an antifungal rather than as an antibacterial. These findings suggest that synthesized nanoscale MgO is promising as a therapeutic candidate for the treatment of candidiasis.

The same results were demonstrated in the study conducted by Amrulloh et al. [10]. In our previous work, MgO nanoparticles were synthesized using moringa leaf extract. The bioactivity testing of the synthesized MgO nanoparticles showed antioxidant activity against DPPH free radicals at a value of 80% with a minimum concentration of MgO nanoparticles used at 200 µg/mL. Based on the MIC values, it is known that MgO nanoparticles exhibit good antibacterial activity against *S. aureus*, *E. faecalis*, *E. coli*, and *S. dysenteriae* (MIC values: 250–500 µg/mL), and stronger antifungal activity against *A. flavus*, *A. niger*, and *C. albicans* (MIC values: 62.5–125 µg/mL).

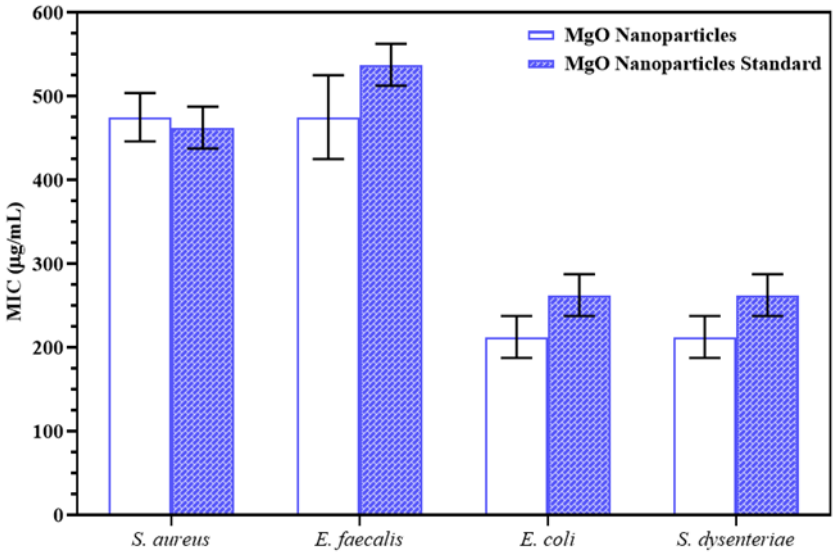

Figure 8. Antibacterial activity of MgO nanoparticles synthesized and MgO nanoparticles standard.

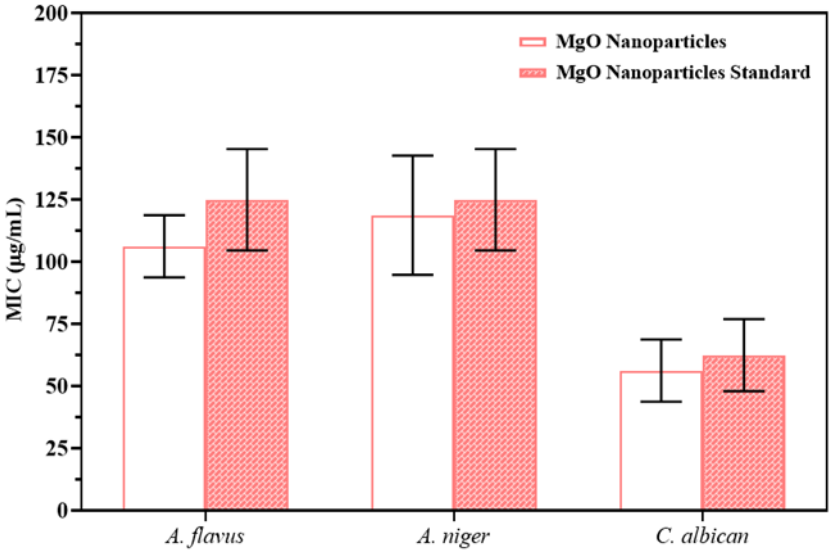

Figure 9. Antifungal activity of the samples against three types of fungi.

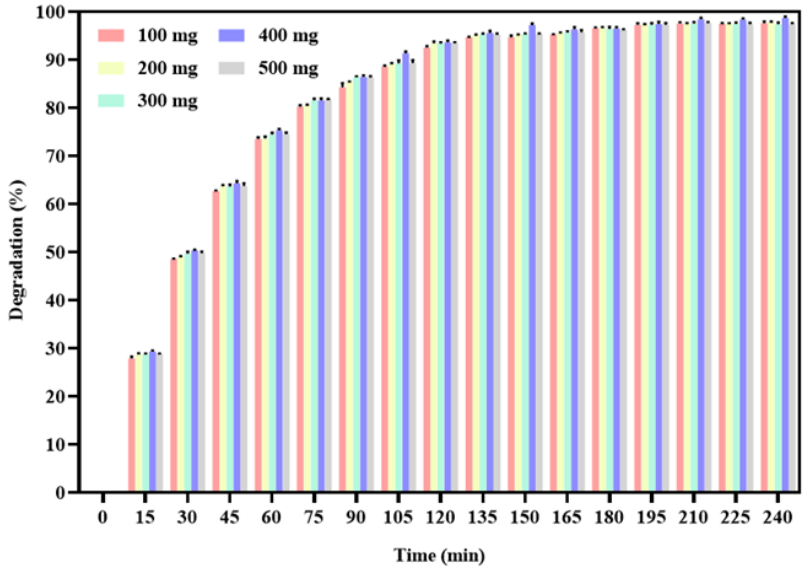

(**a**)

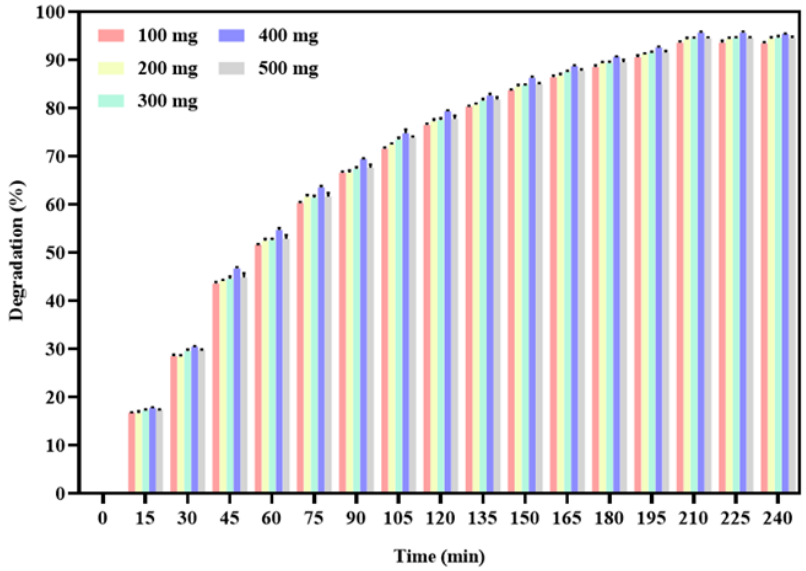

(**b**)

Figure 10. Photocatalytic degradation of (a) MB and (b) RhB dyes.

3.3. Batch Photocatalytic Studies

The photocatalytic degradation of MB and RhB dyes over MgO nanoparticles as photocatalysts is shown in Figures 10(a) and 10(b), respectively. It exhibited significant MB/RhB photocatalysis till 240 min of light enlightenment, which proved that the MB/RhB is stable. After 150 min of illumination, the MgO nanoparticles photocatalyst degraded >97% for MB and >83% for RhB solution. Further, the MgO nanoparticles exhibited an excellent photodegradation of MB dye over RhB. The photodegradation of MB over MgO nanoparticles was found to be 97% after 150 min. The photodegradation of RhB over MgO NPs was found to be 95%, respectively, after 210 min. The MB dye exhibited a higher photodegradation than the RhB dye.

Photodegradation increases with an increase in time, which may be due to an enhancement of the absorption of photons. The effect of nanocomposite dosage on the photodegradation of RhB/MBn dyes was analyzed. The photocatalyst dosage of 400 mg was found to produce maximum photocatalytic degradation and selected for further experimental studies. The different catalyst concentrations from 100 to 500 mg L^{-1} of dye solution indicated that the

MgO NPs have shown an increased photodegradation rate with increasing concentration from 100 to 500 mg L^{-1} for both the dyes. This enhancement is attributed to the high surface area of the metal oxide, increasing with the dosage of the catalyst, leading to a greater number of dye molecules adsorbed on the nanocatalyst surface, rendering it potentially efficient for dye degradation catalysis [38].

In this study, the Eg value of the produced MgO nanoparticle was found to be 4.814 eV. Increased dosage of MgO nanoparticles showed enhanced performance in photocatalytic degradation of MB/RhB dyes. Degradation of MB/RhB dye molecules on the nanocatalyst was facilitated by surface adsorption followed by photocatalytic processes. Under visible light irradiation, electron-hole pair recombination decreased, leading to increased interfacial charge transfer reactions for the degradation of adsorbed MB/RhB molecules. Possible reaction mechanisms in the dye degradation process using MgO nanoparticle catalysts are depicted in Equations (5) – (9).

$$MgO + hv \rightarrow e_{CB}^{-} + h_{VB}^{+} \quad (5)$$

$$e_{CB}^{-} + O_2 \rightarrow O_2^{-} \quad (6)$$

$$2e_{CB}^{-} + O_2^{-} + 2H^{+} \rightarrow \bullet OH + OH^{-} \quad (7)$$

$$h_{VB}^{+} + H_2O \rightarrow H^{+} + \bullet OH \quad (8)$$

$$MB/RhB + \bullet OH \rightarrow CO_2 + H_2O \quad (9)$$

Pachiyappan et al. [26] synthesized MgO nanoparticles using a one-step coprecipitation approach employing *Kappaphycus alvarezii* extract as a stabilizing agent. The synthesized MgO nanoparticles exhibited a cubic crystal structure, confirmed by XRD analysis. UV-DRS was utilized to calculate the Eg value of the MgO nanoparticles, which was found to be 4.71 eV. The MgO nanoparticles demonstrated substantial photocatalytic activity for the degradation of MB (99%) and RhB (95%) dyes under visible light irradiation [26].

4. CONCLUSIONS

The results of this study demonstrated the potential of the electrochemical method for the synthesis of MgO nanoparticles directly from bittern. The formation of MgO nanoparticles was confirmed by the information provided by various characterization techniques applied. The UV-vis was used to calculate the optical band gap and found to be 4.21 eV. Characterisation using the XRD technique confirms the existence of the MgO nanoparticles as crystalline material, while the information regarding the particle size provided by SEM, TEM, EDS, and PSA suggests that the particle sizes are in the range of 25–60 nm. Bioactivity studies reveal that the antibacterial activity as well as antifungal activity of the MgO nanoaprticles synthesised is comparable to those of the NS-MgO standard. The MgO is more effective as an antifungal agent, suggesting its prospective use for the treatment of candidiasis. Additionally, MgO nanoparticles exhibited significant photocatalytic activity in degrading MB and RhB dyes under visible light irradiation, achieving degradation rates of 97% and 95% for both dyes, respectively. Thus, the data obtained from this research can effectively be utilized in large-scale industrial applications during wastewater treatments.

AUTHOR INFORMATION

Corresponding Author

Hanif Amrulloh — Department of Islamic Primary School Teacher Education, Universitas Ma'arif Lampung, Metro-34111 (Indonesia);

orcid.org/0000-0001-7458-9258

Email: amrulloh.h@umala.ac.id

Authors

Chairul Ichsan — Department of Chemistry, Universitas Islam Negeri (UIN) Raden Fatah Palembang, Palembang-30126 (Indonesia);

orcid.org/0000-0002-0878-8133

Wasinton Simanjuntak — Department of Chemistry, Universitas Lampung, Bandar Lampung-35141 (Indonesia);

orcid.org/0000-0001-8152-5084

Oman Zuas — Research Centre for Testing Technology and Standard, Badan Riset dan Inovasi Nasional (BRIN), Tangerang Selatan-15314 (Indonesia);

orcid.org/0000-0002-0101-5277

Yehezkiel Steven Kurniawan — Department of Chemistry, Universitas Gadjah Mada,

Yogyakarta-55281 (Indonesia);
orcid.org/0000-0002-4547-239X
Claudia Maria Simonescu — Department of Analytical Chemistry and Environmental Engineering, National University of Science and Technology POLITEHNICA Bucharest, Bucharest-060042 (Romania);
orcid.org/0000-0002-5308-7344

Author Contributions

Conceptualization, H. A., C. I., W. S., and O. Z.; Methodology, H. A., C. I., and W. S.; Software, C. I. and Y. S. K.; Validation, H. A., W. S. and O. Z.; Formal Analysis, and Investigation, H. A., C. I., and Y. S. K.; Data Curation, H. A., W. S., O. Z., and Y. S. K.; Writing–Original Draft Preparation, H. A. and C. I.; Writing – Review & Editing, W. S., O. Z., Y. S. K. and C. M. S.; Visualization, H. A.; Supervision, W. S., O. Z., and C. M. S.; Funding Acquisition, H. A. and C. I.

Conflicts of Interest

The authors declare no conflict of interest.

ACKNOWLEDGEMENT

This research supported by the Ministry of Religious Affairs Republic Indonesia through collaborative research scheme between universities with number [5378 Tahun 2023].

DECLARATION OF GENERATIVE AI

Not applicable.

REFERENCES

[1] Y. Abdallah, S. O. Ogunyemi, A. Abdelazez, M. Zhang, X. Hong, E. Ibrahim, A. Hossain, H. Fouad, B. Li, and J. Chen. (2019). "The Green Synthesis of MgO Nano-Flowers Using Rosmarinus officinalis L. (Rosemary) and the Antibacterial Activities against Xanthomonas oryzae pv. oryzae". *Biomed Research International.* **2019** : 5620989. 10.1155/2019/5620989.

[2] T. H. Y. Duong, T. N. Nguyen, H. T. Oanh, T. A. Dang Thi, L. N. T. Giang, H. T. Phuong, N. T. Anh, B. M. Nguyen, V. Tran Quang, G. T. Le, and T. V. Nguyen. (2019). "Synthesis of Magnesium Oxide Nanoplates and Their Application in Nitrogen Dioxide and Sulfur Dioxide Adsorption". *Journal of Chemistry.* **2019** : 1-9. 10.1155/2019/4376429.

[3] Z. M. Alaizeri, H. A. Alhadlaq, S. Aldawood, M. J. Akhtar, M. S. Amer, and M. Ahamed. (2021). "Facile Synthesis, Characterization, Photocatalytic Activity, and Cytotoxicity of Ag-Doped MgO Nanoparticles". *Nanomaterials (Basel).* **11** (11). 10.3390/nano11112915.

[4] A. Das, A. C. Mandal, S. Roy, and P. M. G. Nambissan. (2018). "Internal defect structure of calcium doped magnesium oxide nanoparticles studied by positron annihilation spectroscopy". *AIP Advances.* **8** (9). 10.1063/1.5001105.

[5] J. K. Bartley, C. Xu, R. Lloyd, D. I. Enache, D. W. Knight, and G. J. Hutchings. (2012). "Simple method to synthesize high surface area magnesium oxide and its use as a heterogeneous base catalyst". *Applied Catalysis B: Environmental.* **128** : 31-38. 10.1016/j.apcatb.2012.03.036.

[6] N. K. Nga, P. T. Hong, T. D. Lam, and T. Q. Huy. (2013). "A facile synthesis of nanostructured magnesium oxide particles for enhanced adsorption performance in reactive blue 19 removal". *Journal of Colloid and Interface Science.* **398** : 210-6. 10.1016/j.jcis.2013.02.018.

[7] Y. Zheng, L. Cao, G. Xing, Z. Bai, J. Huang, and Z. Zhang. (2019). "Microscale flower-like magnesium oxide for highly efficient photocatalytic degradation of organic dyes in aqueous solution". *RSC Advances.* **9** (13): 7338-7348. 10.1039/c8ra10385b.

[8] V. S. Pinto, D. S. Fini, V. C. Miguel, V. C. Pandolfelli, M. H. Moreira, T. Venâncio, and A. P. Luz. (2020). "Fast drying of high-alumina MgO-bonded refractory castables". *Ceramics International.* **46** (8): 11137-11148. 10.1016/j.ceramint.2020.01.134.

[9] B. Das, S. Moumita, S. Ghosh, M. I. Khan, D. Indira, R. Jayabalan, S. K. Tripathy, A. Mishra, and P. Balasubramanian. (2018). "Biosynthesis of magnesium oxide (MgO)

nanoflakes by using leaf extract of Bauhinia purpurea and evaluation of its antibacterial property against Staphylococcus aureus". *Materials Science and Engineering: C Materials for Biological Applications.* **91** : 436-444. 10.1016/j.msec.2018.05.059.

[10] H. Amrulloh, A. Fatiqin, W. Simanjuntak, H. Afriyani, and A. Annissa. (2021). "Bioactivities of nano-scale magnesium oxide prepared using aqueous extract of Moringa Oleifera leaves as green agent". *Advances in Natural Sciences: Nanoscience and Nanotechnology.* **12** (1). 10.1088/2043-6254/abde39.

[11] E. Behzadi, R. Sarsharzadeh, M. Nouri, F. Attar, K. Akhtari, K. Shahpasand, and M. Falahati. (2019). "Albumin binding and anticancer effect of magnesium oxide nanoparticles". *International Journal of Nanomedicine.* **14** : 257-270. 10.2147/IJN.S186428.

[12] L. Todan, L. Predoana, G. Petcu, S. Preda, D. C. Culita, A. Baran, R. D. Trusca, V. A. Surdu, B. S. Vasile, and A. C. Ianculescu. (2023). "Comparative Study of MgO Nanopowders Prepared by Different Chemical Methods". *Gels.* **9** (8). 10.3390/gels9080624.

[13] F. E. Yunita, N. C. Natasha, E. Sulistiyono, A. R. Rhamdani, A. Hadinata, and E. Yustanti. (2020). "Time and Amplitude Effect on Nano Magnesium Oxide Synthesis from Bittern using Sonochemical Process". *IOP Conference Series: Materials Science and Engineering.* **858** (1). 10.1088/1757-899x/858/1/012045.

[14] H. Cui, X. Wu, Y. Chen, J. Zhang, and R. I. Boughton. (2015). "Influence of copper doping on chlorine adsorption and antibacterial behavior of MgO prepared by co -precipitation method". *Materials Research Bulletin.* **61** : 511-518. 10.1016/j.materresbull.2014.10.067.

[15] A. Fatiqin, H. Amrulloh, and W. Simanjuntak. (2021). "Green synthesis of MgO nanoparticles using Moringa oleifera leaf aqueous extract for antibacterial activity". *Bulletin of the Chemical Society of Ethiopia.* **35** (1): 161-170. 10.4314/bcse.v35i1.14.

[16] J. Hornak. (2021). "Synthesis, Properties, and Selected Technical Applications of Magnesium Oxide Nanoparticles: A Review". *International Journal of Molecular Sciences.* **22** (23). 10.3390/ijms222312752.

[17] H. Amrulloh, W. Simanjuntak, R. T. M. Situmeang, S. L. Sagala, R. Bramawanto, A. Fatiqin, R. Nahrowi, and M. Zuniati. (2020). "Preparation of nano-magnesium oxide from Indonesia local seawater bittern using the electrochemical method". *Inorganic and Nano-Metal Chemistry.* **50** (8): 693-698. 10.1080/24701556.2020.1724146.

[18] H. Amrulloh, Y. S. Kurniawan, C. Ichsan, J. Jelita, W. Simanjuntak, R. T. M. Situmeang, and P. A. Krisbiantoro. (2021). "Highly efficient removal of Pb(II) and Cd(II) ions using magnesium hydroxide nanostructure prepared from seawater bittern by electrochemical method". *Colloids and Surfaces A: Physicochemical and Engineering Aspects.* **631**. 10.1016/j.colsurfa.2021.127687.

[19] N. T. Nguyen, N. Grelling, C. L. Wetteland, R. Rosario, and H. Liu. (2018). "Antimicrobial Activities and Mechanisms of Magnesium Oxide Nanoparticles (nMgO) against Pathogenic Bacteria, Yeasts, and Biofilms". *Scientific Reports.* **8** (1): 16260. 10.1038/s41598-018-34567-5.

[20] N. Kuruthukulangara and I. V. Asharani. (2024). "Photocatalytic degradation of Rhodamine B, a carcinogenic pollutant, by MgO nanoparticles". *Inorganic Chemistry Communications.* **160**. 10.1016/j.inoche.2023.111873.

[21] H. Amrulloh, W. Simanjuntak, and R. T. M. Situmeang. (2017). "Sintesis Mg (OH) 2 dari bittern menggunakan metode elektrokimia". *ALKIMIA: Jurnal Ilmu Kimia dan Terapan.* **1** (1): 10-15.

[22] H. Amrulloh, W. Simanjutak, R. T. M. Situmeang, S. L. Sagala, R. Bramawanto, and R. Nahrowi. (2019). "Effect of Dilution and Electrolysis Time on Recovery of Mg2+ As Mg(OH)2 from Bittern by Electrochemical Method". *The Journal of Pure and Applied*

Chemistry Research. **8** (1): 87-95. 10.21776/ub.jpacr.2019.008.01.455.

[23] N. Andreu, T. Fletcher, N. Krishnan, S. Wiles, and B. D. Robertson. (2012). "Rapid measurement of antituberculosis drug activity in vitro and in macrophages using bioluminescence". *Journal of Antimicrobial Chemotherapy.* **67** (2): 404-14. 10.1093/jac/dkr472.

[24] A. L. Castilho, K. R. Caleffi-Ferracioli, P. H. Canezin, V. L. Dias Siqueira, R. B. de Lima Scodro, and R. F. Cardoso. (2015). "Detection of drug susceptibility in rapidly growing mycobacteria by resazurin broth microdilution assay". *Journal of Microbiological Methods.* **111** : 119-21. 10.1016/j.mimet.2015.02.007.

[25] S. D. Sarker, L. Nahar, and Y. Kumarasamy. (2007). "Microtitre plate-based antibacterial assay incorporating resazurin as an indicator of cell growth, and its application in the in vitro antibacterial screening of phytochemicals". *Methods.* **42** (4): 321-4. 10.1016/j.ymeth.2007.01.006.

[26] J. Pachiyappan, N. Gnanansundaram, S. Sivamani, N. P. B. P. Sankari, N. Senthilnathan, G. A. Kerga, and R. Lakshmipathy. (2022). "Preparation and Characterization of Magnesium Oxide Nanoparticles and Its Application for Photocatalytic Removal of Rhodamine B and Methylene Blue Dyes". *Journal of Nanomaterials.* **2022** : 1-6. 10.1155/2022/6484573.

[27] M. R. Anil Kumar, B. Mahendra, H. P. Nagaswarupa, B. S. Surendra, C. R. Ravikumar, and K. Shetty. (2018). "Photocatalytic Studies of MgO Nano Powder; Synthesized by Green Mediated Route". *Materials Today: Proceedings.* **5** (10): 22221-22228. 10.1016/j.matpr.2018.06.587.

[28] S. A. Kumar, M. Jarvin, S. S. R. Inbanathan, A. Umar, N. P. Lalla, N. Y. Dzade, H. Algadi, Q. I. Rahman, and S. Baskoutas. (2022). "Facile green synthesis of magnesium oxide nanoparticles using tea (Camellia sinensis) extract for efficient photocatalytic degradation of methylene blue dye". *Environmental Technology & Innovation.* **28**. 10.1016/j.eti.2022.102746.

[29] H. Hassanzadeh, A. Salem, and S. Salem. (2023). "Application of ultrasound-assisted technique for production of mesoporous magnesium oxide from solid waste of ductile iron: An alternative method for elimination of surfactants from precipitation process". *Materials Today Communications.* **37**. 10.1016/j.mtcomm.2023.107121.

[30] I. K. Abbas and K. A. Adim. (2023). "Synthesis and characterization of magnesium oxide nanoparticles by atmospheric non-thermal plasma jet". *Kuwait Journal of Science.* **50** (3): 223-230. 10.1016/j.kjs.2023.05.008.

[31] K. Chandra Sekhara Reddy, K. M. Sathish Kumar, and L. S. Reddy Yadav. (2022). "Synthesis and characterization of magnesium oxide nanoparticles using combustion method to study the fuel properties". *Materials Today: Proceedings.* **49** : 797-800. 10.1016/j.matpr.2021.05.297.

[32] J. Sackey, A. K. H. Bashir, A. E. Ameh, M. Nkosi, C. Kaonga, and M. Maaza. (2020). "Date pits extracts assisted synthesis of magnesium oxides nanoparticles and its application towards the photocatalytic degradation of methylene blue". *Journal of King Saud University - Science.* **32** (6): 2767-2776. 10.1016/j.jksus.2020.06.013.

[33] A. Fatiqin, H. Amrulloh, W. Simanjuntak, I. Apriani, R. A. H. T. Amelia, S. Syarifah, R. N. Sunarti, and A. R. P. Raharjeng. (2021). "Characteristics of nano-size MgO prepared using aqueous extract of different parts of Moringa oleifera plant as green synthesis agents". *AIP Conference Proceedings.* **2331** : 040001. 10.1063/5.0041999.

[34] C. Buzea, Pacheco, II, and K. Robbie. (2007). "Nanomaterials and nanoparticles: sources and toxicity". *Biointerphases.* **2** (4): MR17-71. 10.1116/1.2815690.

[35] S. Khorrami, A. Zarepour, and A. Zarrabi. (2019). "Green synthesis of silver nanoparticles at low temperature in a fast pace with unique DPPH radical scavenging and selective cytotoxicity against MCF-7 and BT-20 tumor cell lines". *Biotechnology*

Reports. **24** : e00393. 10.1016/j.btre.2019.e00393.

[36] T. Safawo, B. V. Sandeep, S. Pola, and A. Tadesse. (2018). "Synthesis and characterization of zinc oxide nanoparticles using tuber extract of anchote (Coccinia abyssinica (Lam.) Cong.) for antimicrobial and antioxidant activity assessment". *OpenNano.* **3** : 56-63. 10.1016/j.onano.2018.08.001.

[37] R. Dobrucka. (2017). "Antioxidant and Catalytic Activity of Biosynthesized CuO Nanoparticles Using Extract of Galeopsidis herba". *Journal of Inorganic and Organometallic Polymers and Materials.* **28** (3): 812-819. 10.1007/s10904-017-0750-2.

[38] A. Dey, P. R. Gogate, and Y. M. Gote. (2024). "A review on ultrasound assisted synthesis of metal oxide and doped metal oxide nanocatalysts and subsequent application as photocatalyst for dye degradation". *Environmental Quality Management*. **33** (4): 139-163. 10.1002/tqem.22030.